

# Coronavirus (Covid-19) Classification Using CT Images by Machine Learning Methods

Mücahid Barstuğan<sup>a</sup>, Umut Özkaya<sup>a</sup>, and Şaban Öztürk<sup>b</sup>

<sup>a</sup> Konya Technical University, Electrical and Electronics Engineering, Konya, 42250, Turkey

<sup>b</sup> Amasya University, Electrical and Electronics Engineering, Amasya, 05000, Turkey

## Abstract

This study detected the Coronavirus (COVID-19) disease by implementing artificial learning methods. Coronavirus disease occurs in the lungs and can cause death. The detection process was performed on chest Computed Tomography (CT) images. The training process was implemented by using 32x32 patches that were obtained from CT images. This study includes three phases: The first phase classifies patches by the SVM algorithm without implementing the feature extraction methods. The second phase extracts features on patches by using Grey Level Co-occurrence Matrix (GLCM), Grey Level Run Length Matrix (GLRLM), Grey-Level Size Zone Matrix (GLSZM), Discrete Wavelet Transform (DWT), Fast Fourier Transform (FFT), and Discrete Cosine Transform (DCT) methods and classifies the features extracted. The third phase uses Convolutional Neural Networks (CNN) method to classify the patches. 10-fold cross-validation is implemented in the classification process. The sensitivity, specificity, accuracy, precision, and F-score metrics measure the classification performance. The highest classification accuracy was achieved as 99.15% by the CNN method during the training process. The classification structure, which has the highest classification accuracy, was used during the test performance and had 80.21% mean sensitivity rate, which is the COVID detection performance, on 727 test images.

## Keywords 1

Classification, coronavirus, COVID-19, CT images, deep Learning, feature extraction, machine learning

## 1. Introduction

COVID-19 disease occurred at the end of 2019 at Wuhan region of China. COVID-19 disease shows fever, cough, fatigue, and myalgias in the human body during the early phases [1]. The patients have abnormal situations in their CT chest images. The respiratory problems, heart damages, and secondary infection situations were observed as complications of the disease. The findings show that the COVID-19 virus spreads from person to person. The infected person needs to be treated in the intensive care unit. Infected people have serious respiratory problems. The CT images of the infected people show that

COVID-19 disease has its characteristics. Therefore, clinical experts know the characteristics and need lung CT images to diagnose the COVID-19 in the early phase. The serial CT examinations help clinical experts to understand the occurrence, development, and prognosis of the disease. CT imaging can be sorted into four stages: early stage, progressive stage, severe stage, and dissipative stage [2]. Chest CT imaging modality is one of the key elements during the diagnose of suspected patients [3]. A total of 91,636,996 cases have been diagnosed with COVID-19 infection; 65,524,142 patients have recovered, and 1,961,037 patients have died by January 12, 2021.

Proceedings of RTA-CSIT 2021, May 2021, Tirana, Albania  
EMAIL: [mbarstugan@ktun.edu.tr](mailto:mbarstugan@ktun.edu.tr) (A. 1); [uozkaya@ktun.edu.tr](mailto:uozkaya@ktun.edu.tr) (A. 2); [saban.ozturk@amasya.edu.tr](mailto:saban.ozturk@amasya.edu.tr) (A. 3)



© 2021 Copyright for this paper by its authors. Use permitted under Creative Commons License Attribution 4.0 International (CC BY 4.0).

CEUR Workshop Proceedings (CEUR-WS.org)

The development of computer vision systems supports medical applications such as increasing the image quality, organ segmentation, and organ texture classification. The analysis of time series and tumor characteristics [4], the segmentation and detection [5] of tumor modules are some of the machine learning applications in biomedical image processing field.

In the literature, there are not a detailed study and dataset on coronavirus disease. Xu et al. [6] classified CT images of COVID-19 into three classes as COVID-19, Influenza-A viral pneumonia, and healthy cases. They obtained images from the hospitals in Zhejiang region of China. The dataset consisted of a total of 618 images, which includes 219 images from 110 patients with COVID-19, 224 images of 224 patients with Influenza-A viral pneumonia, and 175 images of 175 healthy people. Their study classified the images with a 3D-dimensional deep learning model and achieved an 87.6% overall classification accuracy. Shan et al. [7] implemented a deep learning-based system for segmenting and quantification of the infected regions as well as the entire lung on chest CT images. They used 249 COVID-19 patients and 300 new COVID-19 patients for validation in their study. The study obtained the Dice similarity coefficient as 91.6%. The regular delineation system often takes 1 to 5 hours; however, their proposed system reduced the delineation time to four minutes. Wang et al. [8] studied 453 CT images of pathogen-confirmed COVID-19 cases along with previously diagnosed with typical viral pneumonia. Their study used the inception migration-learning model to create the algorithm. The study proposed achieved 82.9% validation accuracy and 73.1% test accuracy. Ying et al. [9] used the chest CT images, which were obtained from two different hospitals in China, of 88 patients.

The study proposed a deep learning-based CT diagnosis system to identify COVID-19 patients. The proposed system had 94% classification accuracy. Prabira and Behera [10] proposed a method to detect infected patients by using X-ray scans. The dataset consisted of 100 X-ray images. The method classified X-ray images with the SVM algorithm by using deep features. The proposed method, which was obtained as ResNet50+SVM, has 91.41% classification performance on the MCC metric. There are also some studies, which used lung X-ray scans [11-14]. Besides, some studies [15, 16] used clinical blood test results.

This study created patches from 202 CT images and the samples were labeled as infected/non-infected. The patches were sampled on lung and infected areas. Three different phases were used during the classification of the coronavirus images. The findings showed that the highest classification accuracy was assessed by automatic feature extraction on the images.

This paper is organized as follows. Section 2 analyses the images statistically and visually. Section 3 briefly explains the feature extraction and classification methods. Section 4 presents the classification results. Section 5 concludes the results.

## 2. Material

The dataset was taken from [17]. There are two types of dataset, which were labeled by experts, in [17]. The first dataset has 100 different CT images. The second dataset has 829 CT images, which were obtained from nine patients. The second dataset has non-covid images, also. Table 1 presents the original dataset and patch dataset created.

**Table 1**  
The features of patch dataset

Dataset	Number of images	Number of covid images	Number of training images	Number of test images	Number of infected training patches	Number of non-infected training patches
Dataset 1	100	100	70	30	28047	8843
Dataset 2	829	372	132	697	31307	25670

202 images were used to obtain the training patches. 727 images were used for the test stage. The images in the dataset have acquired from different CT tools. This situation makes the classification process difficult. In some

images, the grey levels are similar to non-infected regions. Also, the grey-level diversion changes dramatically according to the CT tool. Figure 1 shows the infected areas in images that were acquired from different CT tools.

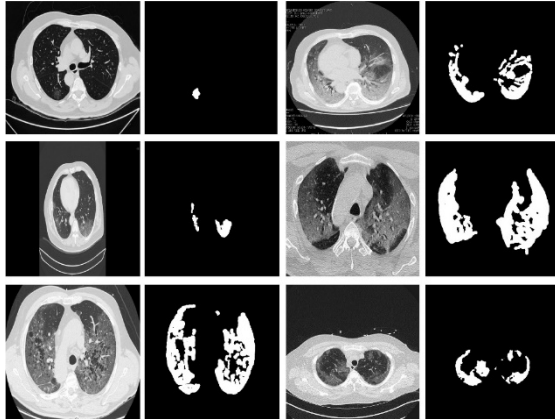


Figure 1: The sample images

### 3. Method

This study classifies the patches into two classes. The first class was created by the patches that were sampled in non-infected areas. The second class was created by the patches that were sampled in infected areas. Figure 2 shows the sample images of infected areas.

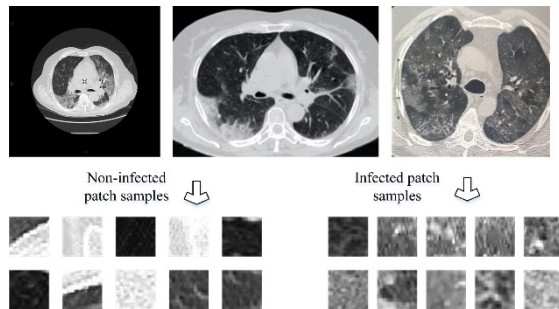


Figure 2: Sample patches for infected and non-infected classes

This study consists of three phases. In the first phase, the patches were transformed into vectors and the SVM classified the vectors. In the second phase, six different feature extraction methods as Grey Level Co-occurrence Matrix (GLCM) [18-20], Grey Level Run Length Matrix (GLRLM) [21], Grey Level Size Zone Matrix (GLSZM) [22] extracted the features. The First Order Statistics (FOS) features were obtained on patches and the transform images of Discrete Wavelet Transform (DWT) [23], Fast Fourier Transform (FFT) [24], and Discrete Cosine Transform (DCT) [25]. The mean, variance, skewness, kurtosis, energy, and entropy values of the

patches were extracted as the FOS features. The SVM [26] method classified all features. During the classification process, the 10-fold cross-validation method was used. In the third phase, a deep learning structure was used to classify the patches. Figure 3 shows the three phases stages of the classification process.

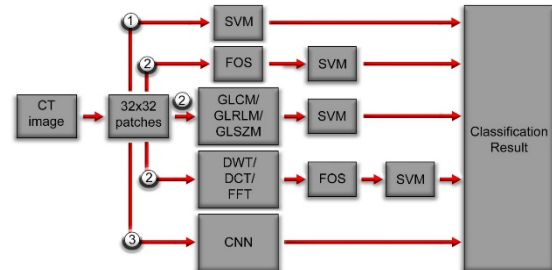
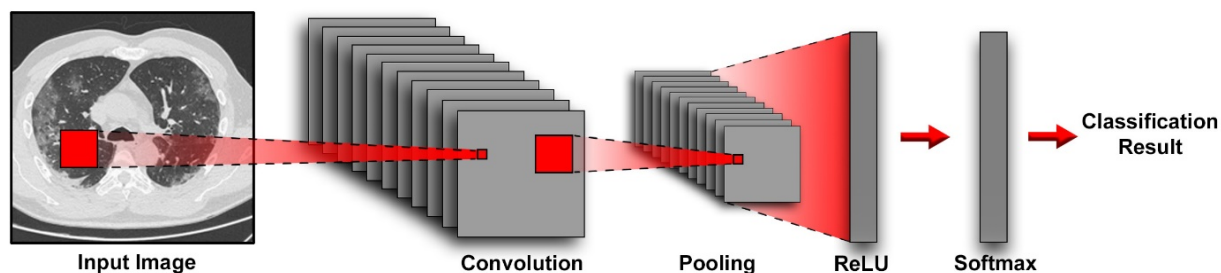


Figure 3: The classification processes for three phases

#### 3.1. The convolutional neural networks

CNN is a biologically-inspired multi-layer perceptron (MLP) structure, which was originated by Hubel and Wiesel who worked on the mammalian visual cortex [27]. Fukushima [28] introduced CNN in 1980, then LeCun et al. [29] progressed in 1989 with a learning deep network study.

CNN has a convolution layer and automatic learning capabilities, which provide widely usage in image classification, object detection, and visual tracking applications. The progress in hardware and parallelization increases this intensive use of CNN [30]. Before the progress, the training process has taken months. After the progress, the training takes several days. The CNN structure includes one or more convolution layers, pooling layers, ReLUs, and softmax regression. The convolutional layer reduces the computational cost by reducing the number of image parameters. The pooling layer is often used to reduce matrix size without losing important features. The ReLU is an activation function and generally used following convolution or pooling layers. Finally, the softmax layer is used for the output value regression. Figure 4 shows the CNN structure used in this study.



**Figure 4:** The CNN structure used in Phase 3

GB DDR4 RAM, and NVIDIA GeForce GTX 1080 graphic card.

## 4. Experimental Results

This study presents a coronavirus classification in three phases. Phase 1 classified the patches without feature extraction. Phase 2 implemented the feature extraction process on all patches and classified the features extracted. Phase 3 used the CNN method to classify the patches. Five different evaluation metrics. These metrics are sensitivity (SEN), specificity (SPE), accuracy (ACC), precision (PRE), and F-score.

All experiments were trained on a computer with Intel Core i7-8700K CPU (3.7 GHz), 32

### 4.1. The classification results of the training process

The dataset for training consists of 202 CT images. The test set consists of 727 images. 59354 infected and 34513 non-infected patches were obtained on 202 training images. These patches were classified by using three phases. Table 2 presents the classification results obtained.

**Table 1**

The features of patch dataset

Phase	Feature Extraction	Classifier Structure	Feature Number	Evaluation Metrics (mean (%) $\pm$ std)				
				SEN	SPE	ACC	PRE	F-score
Phase 1	x	SVM	1024	51.85 $\pm$ 1.8	61.92 $\pm$ 3.1	56.88 $\pm$ 1.3	57.7 $\pm$ 1.7	54.59 $\pm$ 1.2
		FOS-SVM	6	95.32 $\pm$ 0.4	98.12 $\pm$ 0.3	97.09 $\pm$ 0.4	96.72 $\pm$ 0.2	96.01 $\pm$ 0.2
		GLCM-SVM	19	13.22 $\pm$ 0.6	100	68.09 $\pm$ 0.2	100	23.35 $\pm$ 0.8
Phase 2	Manual Feature Extraction	GLRLM-SVM	7	44.85 $\pm$ 0.4	93.72 $\pm$ 0.4	75.75 $\pm$ 0.3	80.62 $\pm$ 1.1	57.63 $\pm$ 0.4
		GLSZM-SVM	13	2.92 $\pm$ 0.2	100	64.31 $\pm$ 0.1	100	5.7 $\pm$ 0.3
		DWT-FOS-SVM	24	65.25 $\pm$ 0.6	92.5 $\pm$ 0.4	82.48 $\pm$ 0.3	83.5 $\pm$ 0.7	73.25 $\pm$ 0.4
		FFT-FOS-SVM	6	65.83 $\pm$ 1.1	90.6 $\pm$ 0.4	81.5 $\pm$ 0.4	80.3 $\pm$ 0.7	72.3 $\pm$
		DCT-FOS-SVM	6	64.54 $\pm$ 0.9	89.96 $\pm$ 0.3	80.61 $\pm$ 0.3	78.9 $\pm$ 0.4	70.99 $\pm$ 0.6

Table 2 shows that the classification accuracy was obtained as 56.88% in Phase 1. The best classification performance in Phase 2 was obtained with the FOS-SVM method as 97.09% with six features. The lowest performances were obtained with the GLSZM-SVM structure, which detected infected patches with too low performance as a 2.92% sensitivity rate. The results show that extracting features increase the classification performance. In Phase 3, a CNN structure, which consists of a convolution layer,

pooling layer, and the softmax layer, was used. Table 3 shows the highest results for Phase 3.

**Table 3**

The classification results for Phase 3

Feature Extraction	Classifier Structure	Accuracy (%)
Automatic Feature Extraction	CNN	99.51

Table 3 shows that the classification accuracy was obtained as 99.15% in Phase 3 during the training process. Table 2 and Table 3 show that the highest classification performance was obtained by the CNN method. Phase 2 achieved maximum classification accuracy as 97.09% with manual feature extraction methods. Phase 3 achieved 99.15% classification accuracy by extracting features automatically.

#### 4.2. The classification results of the test process

This study used the trained structure, which has high classification accuracy, to detect the infected areas in images that were not used during the training stage. Figure 5 presents the test stage implemented.

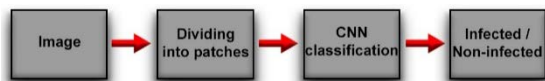


**Figure 5:** The test structure to diagnose the infected

The trained CNN structure classified the 32x32 divided patches, which were not overlapped. During the test stage, a threshold value was determined as “1”. If one patch is classified as infected, the image was classified as infected. If there were not any infected patches in the image, the image was classified as non-infected. When the threshold value was determined as “2”, the classification performance reduced. The reason is that some of images have only one patch size of infected area. When the threshold value was taken bigger than “1”, even these areas were classified as infected, the image was classified as non-infected. This caused classification performance to reduce. 727 test images were classified during test process. Table 4 presents the mean results of test process.

**Table 4**

The classification performance of test process

Method	Evaluation Metrics (%)				
	SEN	SPE	ACC	PRE	F-score
Phase 3	80.21	99.47	98.3	90.8	85.18

Table 4 shows that the proposed method detects the infected images with 80.2% mean sensitivity rate on 727 images. The non-infected patches are classified with a 99.47% mean specificity rate. The CNN structure has 99.15% classification performance during training; however, it has 80.21% performance on test images, which were not used for training.

#### 5. Conclusion

COVID-19 was firstly encountered in Wuhan region in China and has been threatening the public health, trade, and world economy. The virus shows partially similar behaviors with other viral pneumonias. Therefore, the spreading rate of the virus made the situation difficult to be under control. CT imaging results of COVID-19 show different findings according to other clinical studies. Some situations, such as the bronchiectasis, lesion swelling symptoms, and different shadowiness in CT images provide to diagnose COVID-19, easily. This study compared manual feature extraction-based SVM and CNN that automatically extracts features, and achieved that CNN has better performance than SVM method. In this study, the coronavirus image set has a different type of images, which were acquired with different CT tools. Therefore, different feature extraction methods and classifiers were implemented to find the method that separates the infected patches. Table 5 presents the literature studies and their classification performances on different coronavirus dataset.

**Table 5**  
The literature comparison

Study	Method	Dataset	Number of classes	Performance (%)
[6]	3D-deep learning	CT, 618 images	3	87.6
[8]	Migration-learning	CT, 453 images	2	82.9
[10]	ResNet50+SVM	X-ray, 100 images	2	91.41
[13]	COVIDX-Net	X-ray, 50 images	2	90
[16]	XG-boost	Blood Test, 404 samples	2	97
[15]	Random Forest	Blood Test, 49 samples	2	95.12
[30]	Feature Selection and Lasso Regression	Clinical Data	2	84.1
<i>This study</i>	<i>CNN</i>	<i>CT, 727 images</i>	<i>2</i>	<i>80.21</i>

There are different ways to diagnose coronavirus. According to the literature studies in Table 5, CT imaging, X-ray imaging, blood test, and clinical data are used to detect the coronavirus. These datasets were examined by different artificial intelligence methods. This study used a CT dataset and CNN structure. There are not enough CT chest images to train the deep learning methods in the literature. To avoid this problem, the patch classification method was used to overcome the lack of data. If the number of COVID-19 images is increased and a dataset that has data diversity is created, high dimensional deep learning methods may be used, and a classifier structure, which gives higher detection performance, is created.

## 6. Reference

- [1] C. Huang et al., "Clinical features of patients infected with 2019 novel coronavirus in Wuhan, China," vol. 395, no. 10223, pp. 497-506, 2020.
- [2] M. Li et al., "Coronavirus Disease (COVID-19): Spectrum of CT Findings and Temporal Progression of the Disease," 2020.
- [3] L. Fan et al., "Progress and prospect on imaging diagnosis of COVID-19," pp. 1-10, 2020.
- [4] P. Huang et al., "Added value of computer-aided CT image features for early lung cancer diagnosis with small pulmonary nodules: a matched case-control study," vol. 286, no. 1, pp. 286-295, 2018.
- [5] A. Esteva et al., "Dermatologist-level classification of skin cancer with deep neural networks," vol. 542, no. 7639, pp. 115-118, 2017.
- [6] X. Xu et al., "Deep learning system to screen coronavirus disease 2019 pneumonia," 2020.
- [7] F. Shan+ et al., "Lung Infection Quantification of COVID-19 in CT Images with Deep Learning," 2020.
- [8] S. Wang et al., "A deep learning algorithm using CT images to screen for Corona Virus Disease (COVID-19)," 2020.
- [9] Y. Song et al., "Deep learning Enables Accurate Diagnosis of Novel Coronavirus (COVID-19) with CT images," 2020.
- [10] P. K. Sethy and S. K. Behera, "Detection of coronavirus Disease (COVID-19) based on Deep Features," 2020.
- [11] I. D. Apostolopoulos, T. A. J. P. Mpesiana, and E. S. i. Medicine, "Covid-19: automatic detection from x-ray images utilizing transfer learning with convolutional neural networks," p. 1, 2020.
- [12] B. Ghoshal and A. J. a. p. a. Tucker, "Estimating uncertainty and interpretability in deep learning for coronavirus (COVID-19) detection," 2020.
- [13] E. E.-D. Hemdan, M. A. Shouman, and M. E. J. a. p. a. Karar, "COVIDX-Net: A Framework of Deep Learning Classifiers to Diagnose COVID-19 in X-Ray Images," 2020.
- [14] A. Narin, C. Kaya, and Z. J. a. p. a. Pamuk, "Automatic detection of coronavirus disease (COVID-19) using X-ray images and deep convolutional neural networks," 2020.
- [15] J. Wu et al., "Rapid and accurate identification of COVID-19 infection through machine learning based on clinical available blood test results," 2020.
- [16] L. Yan et al., "A machine learning-based model for survival prediction in patients with severe COVID-19 infection," 2020.
- [17] MedSeg.<http://medicalsegmentation.com/covid19/> (accessed 20.04, 2020).
- [18] D. A. J. C. J. o. r. s. Clausi, "An analysis of co-occurrence texture statistics as a function of grey level quantization," vol. 28, no. 1, pp. 45-62, 2002.
- [19] R. M. Haralick, K. Shanmugam, I. H. J. I. T. o. s. Dinstein, man,, and cybernetics, "Textural features for image classification," no. 6, pp. 610-621, 1973.
- [20] L.-K. Soh, C. J. I. T. o. g. Tsatsoulis, and r. sensing, "Texture analysis of SAR sea ice imagery using gray level co-occurrence matrices," vol. 37, no. 2, pp. 780-795, 1999.

- [21] A. S. M. Sohail, P. Bhattacharya, S. P. Mudur, and S. Krishnamurthy, "Local relative GLRLM-based texture feature extraction for classifying ultrasound medical images," in 2011 24th Canadian Conference on Electrical and Computer Engineering (CCECE), 2011: IEEE, pp. 001092-001095.
- [22] G. Thibault, J. Angulo, and F. J. I. T. o. B. E. Meyer, "Advanced statistical matrices for texture characterization: application to cell classification," vol. 61, no. 3, pp. 630-637, 2013.
- [23] M. J. J. I. T. o. s. p. Shensa, "The discrete wavelet transform: wedding the a trous and Mallat algorithms," vol. 40, no. 10, pp. 2464-2482, 1992.
- [24] H. J. Nussbaumer, "The fast Fourier transform," in Fast Fourier Transform and Convolution Algorithms: Springer, 1981, pp. 80-111.
- [25] G. J. S. r. Strang, "The discrete cosine transform," vol. 41, no. 1, pp. 135-147, 1999.
- [26] S. R. Kulkarni and G. J. W. I. R. C. S. Harman, "Statistical learning theory: a tutorial," vol. 3, no. 6, pp. 543-556, 2011.
- [27] D. H. Hubel and T. N. J. T. J. o. p. Wiesel, "Receptive fields and functional architecture of monkey striate cortex," vol. 195, no. 1, pp. 215-243, 1968.
- [28] K. Fukushima, "Neocognitron: A self-organizing neural network model for a mechanism of pattern recognition unaffected by shift in position," *Biological Cybernetics*, vol. 36, no. 4, pp. 193-202, 1980/04/01 1980, doi: 10.1007/BF00344251.
- [29] Y. LeCun et al., "Backpropagation Applied to Handwritten Zip Code Recognition," vol. 1, no. 4, pp. 541-551, 1989, doi: 10.1162/neco.1989.1.4.541.
- [30] C. Feng et al., "A Novel Triage Tool of Artificial Intelligence Assisted Diagnosis Aid System for Suspected COVID-19 pneumonia In Fever Clinics," 2020.